JACS
JOURNAL OF THE AMERICAN CHEMICAL SOCIETY
Article
pubs.acs.org/JACS

# Feedback Response to Selective Depletion of Endogenous Carbon Monoxide in the Blood

Hiroaki Kitagishi,*[,†] Saika Minegishi,[†] Aki Yumura,[†] Shigeru Negi,[‡] Shigeru Taketani,[§] Yoko Amagase,[‡] Yumiko Mizukawa,[‡] Tetsuro Urushidani,[‡] Yukio Sugiura,[‡] and Koji Kano[†]

[†]Department of Molecular Chemistry and Biochemistry, Faculty of Science and Engineering, Doshisha University, Kyotanabe, Kyoto 610-0321, Japan

[‡]Faculty of Pharmaceutical Sciences, Doshisha Women's College of Liberal Arts, Kyotanabe, Kyoto 610-0395, Japan

[§]Department of Microbiology, Kansai Medical University, Hirakata, Osaka 573-1010, Japan

Supporting Information

**ABSTRACT:** The physiological roles of endogenous carbon monoxide (CO) have not been fully understood because of the difficulty in preparing a loss-of-function phenotype of this molecule. Here, we have utilized in vivo CO receptors, hemoCDs, which are the supramolecular 1:1 inclusion complexes of *meso*-tetrakis(4-sulfonatophenyl)porphinatoiron-(II) with per-*O*-methylated $\beta$-cyclodextrin dimers. Three types of hemoCDs (hemoCD1, hemoCD2, and hemoCD3) that exhibit different CO-affinities have been tested as CO-depleting agents in vivo. Intraperitoneally administered hemoCD bound endogenous CO within the murine circulation, and was excreted in the urine along with CO in an affinity-dependent manner. The sufficient administration of hemoCD that has higher CO-affinity than hemoglobin (Hb) produced a pseudoknockdown state of CO in the mouse in which heme oxygenase-1 (HO-1) was markedly induced in the liver, causing the acceleration of endogenous CO production to maintain constant CO-Hb levels in the blood. The contents of free hemin and bilirubin in the blood plasma of the treated mice significantly increased upon removal of endogenous CO by hemoCD. Thus, a homeostatic feedback model for the CO/HO-1 system was proposed as follows: HemoCD primarily removes CO from cell-free CO-Hb. The resulting oxy-Hb is quickly oxidized to met-Hb by oxidant(s) such as hydrogen peroxide in the blood plasma. The met-Hb readily releases free hemin that directly induces HO-1 in the liver, which metabolizes the hemin into iron, biliverdin, and CO. The newly produced CO binds to ferrous Hb to form CO-Hb as an oxidation-resistant state. Overall, the present system revealed the regulatory role of CO for maintaining the ferrous/ferric balance of Hb in the blood.

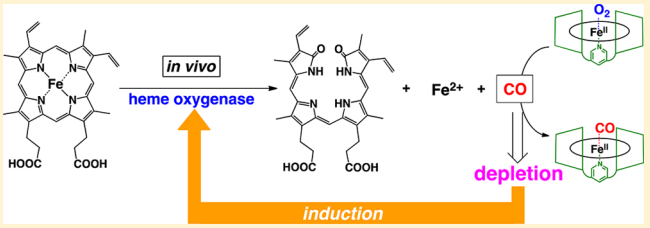


## INTRODUCTION

Carbon monoxide (CO) is continuously produced in mammalian organisms.[1] In the human body, about 10 mL of CO is produced per day through natural metabolic processes.[2] The major endogenous process of CO production (ca. 86%) is the degradation reaction of a heme prosthetic group, while a minor amount of CO arises from lipid oxidation.[1,2] Therefore, the main precursor of CO in living organisms is hemin, the ferric form of the heme prosthetic group (Figure 1). Hemin is released from aged heme proteins, which arise primarily from cell-free hemoglobin (Hb) leaked from senescent red blood cells (RBCs).[3,4] While Hb in RBCs exists in its ferrous form, cell-free Hb is rapidly oxidized to its ferric form (met-Hb) by reactive oxygen species (ROS) existing in the blood.[3,4] The cell-free met-Hb easily dissociates to hemin and apo-globin, and serum proteins such as hemopexin transport hemin into cells.[3−5] The enzymatic reaction of heme oxygenase (HO) in the cells causes the degradation of hemin to generate CO, biliverdin, and iron (Figure 1).[1−5] The endogenously produced CO can then diffuse back out through the cell membrane. Most

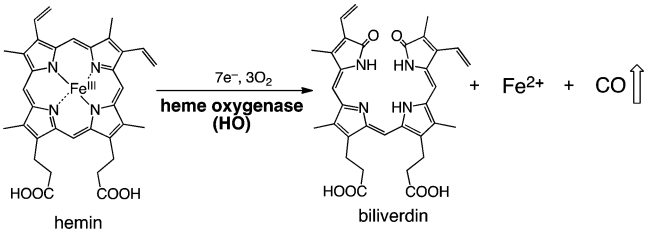


**Figure 1.** Metabolic degradation of hemin by a heme oxygenase enzyme (HO) to endogenously produce biliverdin, $Fe^{2+}$, and CO.

of the endogenously produced CO (ca. 80%) circulates as CO-Hb in the blood;[6,7] thus, normal human blood contains a fraction of CO-Hb (1.2 ± 0.3% of total Hb) even in nonsmokers.[8] Since the finding that CO at low concentration (below 500 ppm) exerts a remarkable protective effect against inflammation in cardiac transplant[9] and ischemia/reperfusion

**Received:** February 29, 2016
**Published:** April 8, 2016





DOI: 10.1021/jacs.6b02211
J. Am. Chem. Soc. 2016, 138, 5417−5425

models,[10] much effort has been directed toward the therapeutic use of CO as an anti-inflammatory agent.[1,2,11,12] In particular, water-soluble, nontoxic metal carbonyl complexes have been developed as agents for the controlled release of CO in vivo.[11−15]

The functional mechanisms of CO in biological systems have been extensively studied over the past two decades,[1,2,12] but are not fully understood. In vitro as well as in vivo studies have clearly revealed that CO at low concentration inhibits the production of stress-induced pro-inflammatory cytokines through several signaling pathways, resulting in an anti-inflammatory effect.[16−19] Furthermore, the discovery of CO-responsive transcriptional factors such as neuronal PAS domain 2[20] and CooA[21] has strongly suggested the existence of gene expression regulatory systems controlled by intracellular CO.[22,23] However, the majority of endogenous CO primarily circulates in the blood as CO-Hb and is not retained within cells. Although the intracellular CO has been demonstrated to function as a signaling molecule, the role of endogenous CO in the blood remains unclear. To understand the overall role of endogenous CO, the phenotypes of HO-knockout mice have been characterized.[1,24,25] Upon genetic deletion as well as chemical inhibition of HO activity, however, redundant hemin might accumulate in the blood and/or in cells. The primary role of endogenous CO itself in living systems remains uncertain owing to the difficulty in generating a loss-of-function phenotype of this gaseous molecule.

In the present study, we developed a selective in vivo CO-depletion system without the requirement for genetic manipulation. The key materials are the synthetic CO-receptors, hemoCDs, which are supramolecular 1:1 inclusion complexes of *meso*-tetrakis(4-sulfonatophenyl)porphinatoiron(II) ($Fe^{II}$TPPS) with per-*O*-methylated $\beta$-cyclodextrin dimers (Figure 2). We had designed hemoCDs as synthetic myoglobin (Mb) and/or Hb model complexes that reversibly bind molecular oxygen ($O_2$) in aqueous solution.[26] A series of hemoCDs (hemoCD1,[26,27] hemoCD2,[28] and hemoCD3,[29] Figure 2) are reported as the model complexes showing different $O_2$ and CO binding affinities (Table 1). Since the CO binding affinity of hemoCD1 was much higher than that of Hb

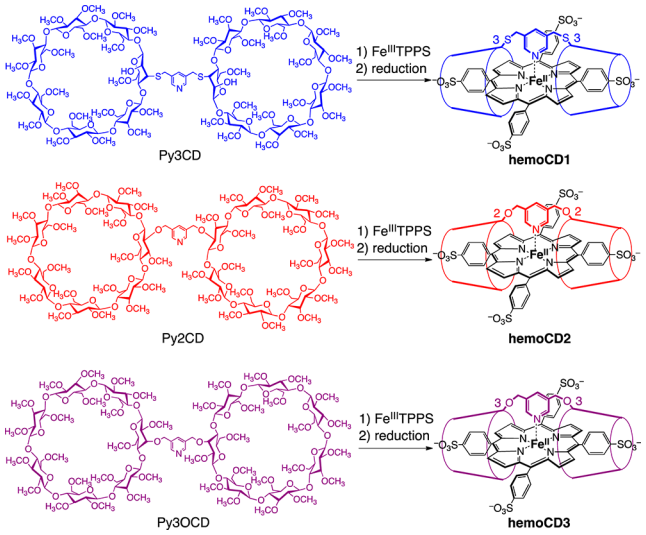


**Figure 2.** Structures of the hemoCD1, hemoCD2, and hemoCD3 complexes used in this study as supramolecular CO-depleting agents that function in vivo.

**Table 1. $O_2$ and CO Binding Affinities ($P_{1/2}^{L}$, L = $O_2$ or CO, Torr)[a] and Half-Lives for the Autoxidation of the Oxygenated Complexes ($t_{1/2}^{O2}$, h) in Aqueous Phosphate Buffer Solution at 25 °C**

| | $P_{1/2}^{O2}$/Torr | $10^3P_{1/2}^{CO}$/Torr | $t_{1/2}^{O2}$/h | ref. |
|---|---|---|---|---|
| hemoCD1 | 10 | 0.015 | 30 | 27 |
| hemoCD2 | 176 | 16 | >100 | 28 |
| hemoCD3 | 18 | 0.56 | 53 | 29 |
| Hb, human, R-state | 0.22 | 1.4 | >60 | 30 |

[a] $P_{1/2}^{L}$ (L = $O_2$ or CO) represents the partial pressure of $O_2$ or CO at which half of the ferrous complexes are bound by $O_2$ or CO.

in the R-state,[27,30] the $O_2$ complex of hemoCD1 (oxy-hemoCD1) intravenously injected to rats was capable of capturing endogenous CO in the blood of the animals.[31,32] The supramolecular structure of hemoCD1 was so stable that no dissociation to its components was observed in the blood or in the urine.[31] Throughout this study, we used oxy-hemoCDs as the CO-removal agents, which captured CO from CO-Hb through the ligand exchange reaction between $O_2$ and CO. The present study showed, for the first time, that the depletion of CO from the blood accelerates the endogenous production of CO by inducing HO-1, an inducible isoform of the HO enzymes. Accordingly, we propose a homeostatic feedback model for the endogenous CO/HO-1 system.

## RESULTS AND DISCUSSION

**Sample Preparation.** The solution of hemoCD in phosphate buffer saline (PBS) for administration to mice was prepared as follows: The solution of met-hemoCD, which contained $Fe^{III}$TPPS and 1.2 equiv of a CD dimer (Py3CD,[27] Py2CD,[28] or Py3OCD,[29] Figure 2) in PBS, was reduced to its ferrous form (hemoCD) by excess $Na_2S_2O_4$. The excess $Na_2S_2O_4$ and its decomposed products were then removed by passing the solution through a Sephadex G-25 desalting column. Under aerobic conditions, the ferrous complex was spontaneously oxygenated to form an $O_2$ complex (oxy-hemoCD) during the treatment. The eluted solution containing ferrous hemoCD in PBS was immediately used for administration to subject animals to minimize its autoxidation (Table 1).

Before the in vivo experiments, the CO-removal ability of each hemoCD from CO-Hb in vitro was assessed using the competitive reaction assay (Figure S1). According to the CO-affinities listed in Table 1, hemoCD1 and hemoCD3 removed CO quantitatively from equimolar CO-Hb, whereas only a fraction of CO was removed from CO-Hb by hemoCD2. In the reaction with hemoCD, CO-Hb was converted to oxy-Hb owing to the ligand exchange between CO and $O_2$.

**Pharmacokinetic Study.** To investigate how much hemoCD was necessary for complete removal of endogenous CO in the blood, the solutions of hemoCD1 (0.15 mL) at different concentrations (0.5, 1.0, and 1.5 mM) were intraperitoneally administrated to male C57BL/6N mice. To avoid biological reactions induced by anesthesia, we utilized intraperitoneal administration to the unanesthetized SPF mice. Following the administration, red-colored urine was spontaneously excreted owing to the renal clearance of hemoCD1. Figure 3a shows a typical example of the UV−vis spectrum of the urine. The Soret band that was sharper than that of oxy-hemoCD1 indicated the existence of CO-bound hemoCD1 (CO-hemoCD1) in the urine. This observation represents the


DOI: 10.1021/jacs.6b02211
J. Am. Chem. Soc. 2016, 138, 5417−5425

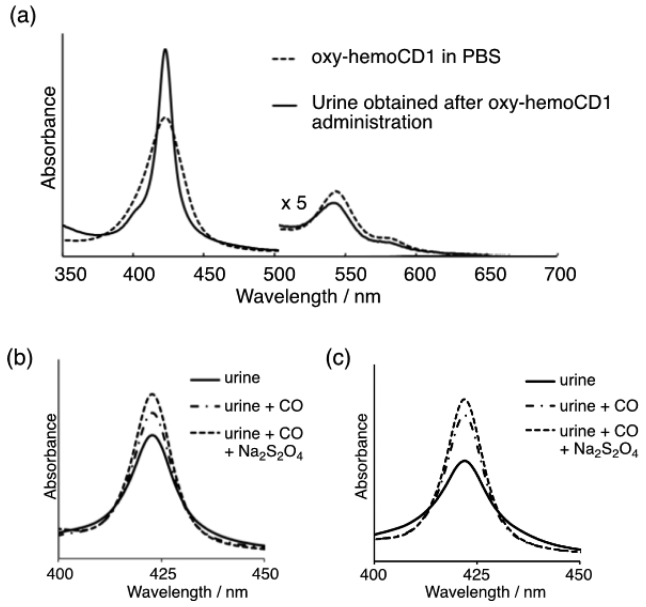


**Figure 3.** UV−vis spectral characterization of the urine. (a) UV−vis spectra of oxy-hemoCD1 in PBS (dashed line) and the urine solution diluted in PBS (solid line). The urine was obtained spontaneously after the administration of oxy-hemoCD1. (b, c) UV−vis spectra of the urine solutions obtained from the hemoCD1-treated mice (b, 0.5 mM, 0.15 mL; c, 1.0 mM, 0.15 mL) before and after the additions of CO and CO/excess $Na_2S_2O_4$. From the absorbances in these spectra, the amount of total hemoCD1 ($M_{hemoCD1}$) and the molar fractions of CO-, oxy-, and met-hemoCD1 in the urine were determined.

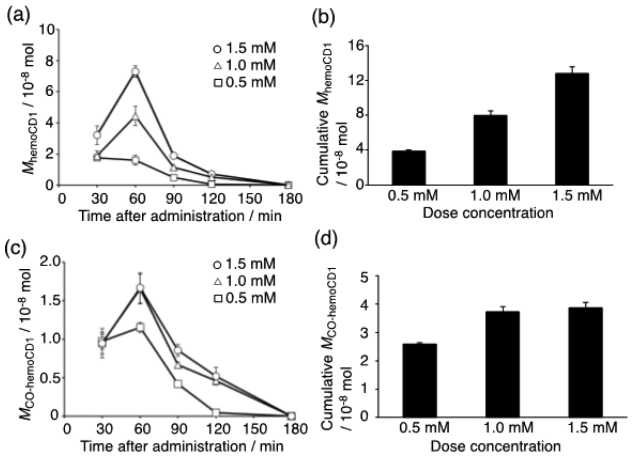


**Figure 4.** Urinary excretion profiles for the mice after intraperitoneal administration of hemoCD1 (0.5, 1.0, or 1.5 mM in PBS, 0.15 mL each). (a) Changes in the amount of hemoCD1 excreted in the urine ($M_{hemoCD1}$, mol) as a function of time; (b) the cumulative value of $M_{hemoCD1}$ for 180 min after the administration; (c) changes in the amount of CO-hemoCD1 excreted in the urine ($M_{CO\text{-}hemoCD1}$, mol) as a function of time; and (d) the cumulative value of $M_{CO\text{-}hemoCD1}$ for 180 min after the administration. Each bar represents the means ± SE ($n$ = 3 mice per time point).

following processes: (1) absorption of hemoCD1 from the peritoneal cavity into the bloodstream, (2) ligand exchange of $O_2$ in oxy-hemoCD1 with endogenous CO, and (3) the glomerular filtration of CO-hemoCD1 into the urine. The transfer of hemoCD1 from the bloodstream into the urine accompanied by endogenous CO has been previously confirmed by resonance Raman spectroscopy as well as UV−vis spectroscopy.[31] Endogenous nitric oxide (NO) was considered not to bind to hemoCD1 in the blood as previously studied using rats.[31] Therefore, the urine contained three different states of hemoCD1, i.e., oxy-hemoCD1, CO-hemoCD1, and met-hemoCD1; the molar fractions of these components were determined using the CO/$Na_2S_2O_4$ assay.[31−33] Figures 3b and 3c show the typical UV−vis spectral changes of the urine solutions before and after the successive additions of CO and $Na_2S_2O_4$. Addition of CO gas into the urine sample caused an increase in the absorbance at 422 nm, owing to the conversion of residual oxy-hemoCD1 to CO-hemoCD1. Subsequent addition of $Na_2S_2O_4$ caused further enhancement of the absorption band at 422 nm, indicating that the urine included met-hemoCD1 as well.

Figure 4a shows the time courses of the excreted hemoCD1 ($M_{hemoCD1}$) after the intraperitoneal administration of hemoCD1 (applied doses: 0.5, 1.0, and 1.5 mM in PBS, 0.15 mL each). The time courses for $M_{hemoCD1}$ showed a dependency on the dose concentration. The administered hemoCD1 completely disappeared at 180 min; this rapid renal clearance was also observed for rats,[31,32] in which ca. 80% of intravenously administered hemoCD1 was transferred into the urinary bladder. In the present study, an average of 53 ± 5% administered hemoCD1 was spontaneously excreted in the urine after intraperitoneal injection in mice, as evaluated from the cumulative $M_{hemoCD1}$ values (Figure 4b). The renal clearance ratio was independent of its dose concentrations (0.5, 1.0, and 1.5 mM), whereas the molar fractions of the individual components (oxy-, CO-, and met-hemoCD1) in the total hemoCD1 in the urine showed strong dose-dependency (Figure S2); the fraction of the CO complex was lower when hemoCD1 at higher concentration was administered to the mice. The time-courses of the amount of the CO complex in the urine ($M_{CO\text{-}hemoCD1}$), which is equal to the amount of endogenous CO removed from the body, are shown in Figure 4c. The data showed no differences at the 1.0 and 1.5 mM applied doses. The cumulative $M_{CO\text{-}hemoCD1}$ values (Figure 4d) indicated that (3.8 ± 0.2) × $10^{-8}$ mol of endogenous CO was removed by hemoCD1, which saturated at doses over 1.0 mM. The results indicate that the removable endogenous CO was completely excreted in the urine as CO-hemoCD1 when over 1.0 mM hemoCD1 (0.15 mL) was administered to the mouse.

HemoCD2 and hemoCD3, which show lower CO-binding affinities than hemoCD1 (Table 1), were administered to mice in the same manner as hemoCD1. Figure 5 shows the comparison of the pharmacokinetic profiles between hemoCD1, hemoCD2, and hemoCD3 (applied doses: 1.0 mM, 0.15 mL each). There was no difference in the amounts of the excreted hemoCD molecules ($M_{hemoCD}$) between the complexes (Figure 5a and b). HemoCD2, having a lower CO binding affinity than Hb, insufficiently removed endogenous CO whereas hemoCD3 removed similar amounts of CO as hemoCD1 (Figure 5c and d). The results indicated that a constant amount of endogenous CO could be removed by sufficient administration of hemoCDs that exhibit higher CO binding affinities than Hb.

The CO-Hb contents in the blood were measured after the administration of hemoCDs to mice as a function of time (Figure 6). In the control mice (PBS), the fraction of CO-Hb (%) in the total Hb was found to be ca. 0.2%, which is consistent with the reported value for the mouse blood.[34] At 30 min after the administration of hemoCD1 or hemoCD3, the


DOI: 10.1021/jacs.6b02211
J. Am. Chem. Soc. 2016, 138, 5417−5425

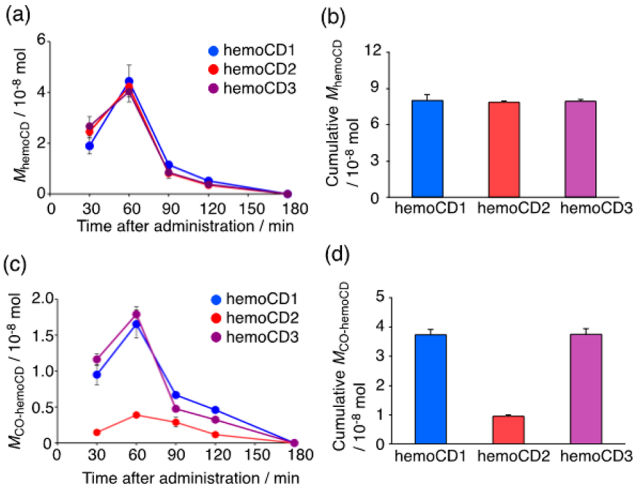


**Figure 5.** Urinary excretion profiles for the mice after intraperitoneal administration of hemoCD1, hemoCD2, or hemoCD3 (1.0 mM in PBS, 0.15 mL each). (a) Changes in the total amount of hemoCD excreted in the urine ($M_{hemoCD}$, mol) as a function of time; (b) the cumulative value of $M_{hemoCD}$ for 180 min after the administration; (c) changes in the amount of CO-hemoCD1 excreted in the urine ($M_{CO\text{-}hemoCD}$, mol) as a function of time; and (d) the cumulative value of $M_{CO\text{-}hemoCD}$ for 180 min after the administration. Each bar represents the means ± SE ($n$ = 3 mice per time point).

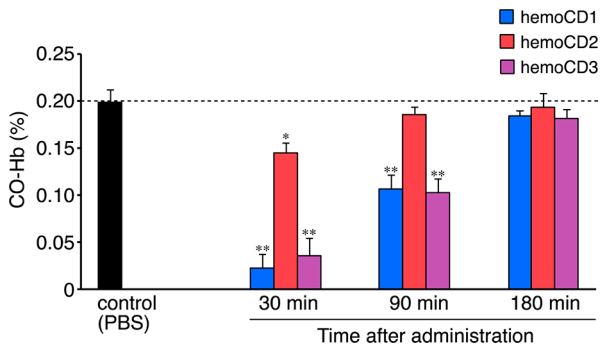


**Figure 6.** Time-courses of the fraction of CO-Hb (%) in the whole blood of the mice after the intraperitoneal administration of hemoCD1, hemoCD2, or hemoCD3 (1.0 mM, 0.15 mL each). The control data were obtained from the blood of mice at 30 min after the intraperitoneal administration of PBS (0.15 mL). Each bar represents the means ± SE ($n$ = 3 mice per time point). An asterisk denotes statistical significance: *$P$ < 0.05, **$P$ < 0.01, as compared to the controls.

value was drastically reduced to below 0.03%, indicating that these hemoCDs removed endogenous CO from CO-Hb circulating in the blood. On the other hand, the effect of hemoCD2 was small, owing to its lower CO affinity than Hb (Table 1). The CO-Hb content returned smoothly to a normal level (ca. 0.2%) at 180 min after hemoCD administration, at which the dosed hemoCDs disappeared from the body (Figure 5a). Such rapid recovery of the CO-Hb content suggested that the endogenous CO was newly produced to compensate for the lack of CO in the blood.

**Induction of HO-1 by CO-Depletion.** The compensative production of endogenous CO that occurred in the hemoCD-treated mouse strongly suggested an enhancement of the enzymatic activity of HO. The HO enzyme is classified mainly as two isozymes, inducible HO-1 and constitutive HO-2.[1,2] Therefore, the mRNA levels of HO-1 (*Hmox1*) and HO-2 (*Hmox2*) in the livers of mice were examined using a quantitative PCR method. The solution of hemoCD (1.0 mM, 0.15 mL) was administered to mice and total RNA was then extracted from the liver at 30, 90, and 180 min after the administration. Iron-free hemoCD1 (a mixed solution of 5,10,15,20-tetrakis(4-sulfonatophenyl)porphyrin (TPPS) and Py3CD, hereafter abbreviated as Fb-hemoCD1) was similarly administered to another mouse as a negative control. Met-hemoCD, a ferric form of hemoCD, could not be used as the negative control because it was partially reduced to its ferrous form during its circulation in the bloodstream.[29,31] The intraperitoneally administered Fb-hemoCD1 was excreted in the urine without showing any UV−vis spectral change (Figure S3), indicating that no dissociation and no specific interaction with biomolecules occurred during its circulation and excretion.

*Hmox1* expression levels were significantly enhanced in the mice treated by hemoCDs (Figure 7a). At 90 min after

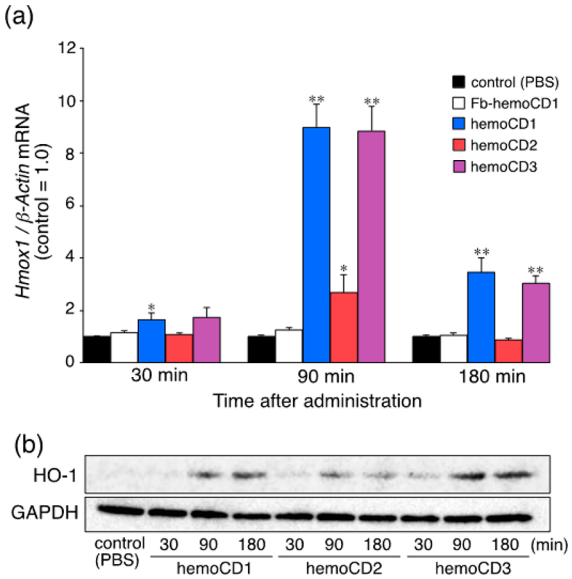


**Figure 7.** Induction of HO-1 following hemoCD administration. (a) Relative mRNA expression levels of HO-1 in the mice liver after the intraperitoneal administration of hemoCD1, hemoCD2, or hemoCD3 (1.0 mM, 0.15 mL each). PBS and Fb-hemoCD1 were similarly administered as controls. Each bar represents the means ± SE ($n$ = 3 mice per group). An asterisk denotes statistical significance, *$P$ < 0.05, **$P$ < 0.01, as compared to the controls. (d) Western blot analysis of the liver using an anti-HO-1 antibody at 30, 90, and 180 min after the administration of hemoCD1, hemoCD2, or hemoCD3. The samples for the control were obtained from the mice at 30 min after the intraperitoneal administration of PBS (0.15 mL).

hemoCD1 or hemoCD3 injection, ca. 9-fold higher mRNA expression was observed as compared with the controls (PBS and Fb-hemoCD1). On the other hand, relatively weak induction (ca. 2.5-fold) was observed in the case of hemoCD2, indicating that *Hmox1* induction was dependent on the respective CO affinities of the hemoCDs. The enhanced mRNA gradually returned to a normal level. The time-courses of the transcriptional responses of *Hmox1* followed the depletion of CO-Hb in the blood as shown in Figure 6; the stronger depletion of CO-Hb in the blood caused a larger *Hmox1* mRNA induction in the mouse liver. In contrast, *Hmox2* expression levels were not affected by hemoCD administration (Figure S4).


DOI: 10.1021/jacs.6b02211
J. Am. Chem. Soc. 2016, 138, 5417−5425

The induction of mRNA in the mouse liver correlated with HO-1 protein expression, as confirmed by Western blot analysis using an anti-HO-1 antibody (Figure 7b). HO-1 protein began to accumulate in the liver at 90 min after the hemoCD dosing. The accumulated HO-1 protein is able to produce additional endogenous CO via the enzymatic degradation of hemin, leading to recovery of the reduced CO-Hb level in the blood as shown in Figure 6.

**In Vitro Analysis.** The expression level of *Hmox1* was also measured in vitro using mammalian hepatoma cells (HepG2) following incubation with hemoCD. We previously found that Fb-hemoCD cannot penetrate the cell membrane.[35] Therefore, it is reasonable to assume that hemoCD exists in the culture medium. Such conditions are similar to those of the in vivo experiments, wherein hemoCD circulated in the bloodstream without having any specific interactions with the surrounding cells. Unlike the in vivo experiments, however, the ferrous hemoCD1 (oxy-hemoCD1) in the culture medium did not affect the expression level of *Hmox1* in the HepG2 cells (Figure 8a). The individual components, i.e., met-hemoCD1, Fe$^{III}$TPPS, and Py3CD, also did not induce *Hmox1*. It has been demonstrated that the natural biologic system does not recognize *meso*-tetraphenylporphinatoiron (FeTPP) derivatives as heme cofactor analogues because of the nonplanar structure of their peripheral phenyl substituents.[36,37] In addition, hemoCD did not exhibit any cytotoxic and hemolytic activities.[38] Therefore, the induction of HO-1 observed in vivo cannot be ascribed to the direct interaction of the hemoCD molecules with the cells. Instead, the induction of HO-1 in vivo is attributable to the removal of endogenous CO by hemoCD in the blood.

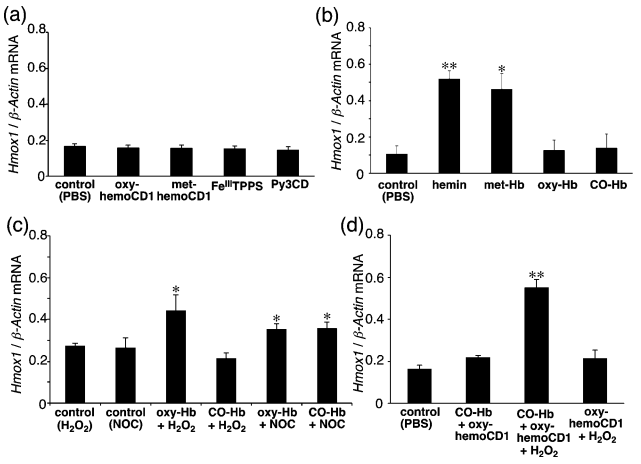


**Figure 8.** In vitro RT-PCR analysis of mRNA expression levels of HO-1 in HepG2 cells. Cells were incubated for 2 h with the following components prior to RT-PCR analysis: (a) Oxy-hemoCD1 (10 $\mu$M), met-hemoCD1 (10 $\mu$M), Fe$^{III}$TPPS (10 $\mu$M), or Py3CD (10 $\mu$M); (b) hemin (10 $\mu$M), met-Hb (100 $\mu$M), oxy-Hb (100 $\mu$M), or CO-Hb (100 $\mu$M); (c) $H_2O_2$ (200 $\mu$M), NOC (a NO gas releasing agent, 250 $\mu$M), oxy-Hb + $H_2O_2$ (100 $\mu$M + 200 $\mu$M), CO-Hb + $H_2O_2$ (100 $\mu$M + 200 $\mu$M), oxy-Hb + NOC (100 $\mu$M + 250 $\mu$M), or CO-Hb + NOC (100 $\mu$M + 250 $\mu$M); or (d) CO-Hb + oxy-hemoCD1 (100 $\mu$M + 300 $\mu$M), CO-Hb + oxy-hemoCD1 + $H_2O_2$ (100 $\mu$M + 300 $\mu$M + 200 $\mu$M), or oxy-hemoCD1 + $H_2O_2$ (300 $\mu$M + 200 $\mu$M). Each bar represents the means ± SE ($n$ = 3−7 experiments per group). The asterisks denote statistical significance, *$P$ < 0.05, **$P$ < 0.01, as compared to the controls.

As previously reported,[39] a strong *Hmox1* induction occurred in the HepG2 cells when they were incubated with hemin (Figure 8b). Hemin (Figure 1) is the substrate of HO-1 and thus a potent inducer for HO-1.[40] Hemin complexed with the globin protein (i.e., met-Hb) also induced *Hmox1*, whereas ferrous Hbs (oxy-Hb and CO-Hb) did not (Figure 8b). Ferrous heme is captured by globin protein more tightly than the ferric state (i.e., hemin).[41] Therefore, met-Hb tends to partly dissociate to hemin and apo-globin in the culture medium. The released hemin from met-Hb in turn might penetrate the cell membrane to induce *Hmox1* in the cells. The release of hemin from met-Hb is considered to take place more efficiently in the bloodstream in vivo because of the presence of the intracellular transportation system for free hemin in the blood plasma.[5]

We hypothesized that the oxidation of ferrous Hb to met-Hb is the key reaction in the HO-1 induction observed in the CO-Hb depleted mice. The intravascular oxidation of ferrous Hb to met-Hb is known to be promoted by active oxidants such as hydrogen peroxide ($H_2O_2$) and NO in the blood,[42] whose plasma concentrations range from 20−60 $\mu$M for $H_2O_2$[43] and 0.003−1 $\mu$M for NO.[44] Ferrous Hb is oxidized by $H_2O_2$ to met-Hb via ferryl intermediates.[45] $H_2O_2$ oxidizes deoxy-Hb ca.100-times more rapidly than oxy-Hb.[46] Because CO binds more strongly to the ferrous center of Hb than does $O_2$, the oxidation of CO-Hb by $H_2O_2$ is much slower than that of oxy-Hb, as shown in Figure S5. In other words, CO suppresses the $H_2O_2$-promoted oxidation of ferrous Hb to met-Hb. Such suppression has been previously proposed by Soares and Mota,[47] who reported that exogenously inhaled CO functions very effectively to reduce the generation of free hemin in the plasma of malaria-infected model mice.

On the other hand, NO promoted the oxidation of both oxy-Hb and CO-Hb to met-Hb with similar rates (Figure S6). NO binds to ferrous Hb more strongly than $O_2$ and CO,[48] and the resulting NO-Hb is readily oxidized to met-Hb under aerobic conditions.[49] The difference between $H_2O_2$ and NO in their reactivity to ferrous Hb (oxy- and CO-Hb) was clearly reflected in the *Hmox1* expression in the HepG2 cells (Figure 8c). *Hmox1* was induced when the oxidation of ferrous Hb by $H_2O_2$ or NO occurred in the culture medium. In contrast, CO-Hb did not induce *Hmox1* even in the presence of $H_2O_2$ (Figure 8c). When the CO ligand of CO-Hb was removed by oxy-hemoCD1 in the culture medium, *Hmox1* was significantly induced by $H_2O_2$ (Figure 8d). These results indicated that the removal of CO from CO-Hb caused an accumulation of met-Hb via the oxidation of oxy-Hb by $H_2O_2$, which led to the release of free hemin that subsequently induced *Hmox1*.

**Blood Plasma Analysis.** To determine whether the CO-depletion in the blood caused an accumulation of free hemin, blood samples were collected from the mice at 30, 90, and 180 min after the intraperitoneal administration of hemoCD1 (1.0 mM, 0.15 mL) and analyzed. The increase of met-Hb in the blood of the CO-depleted mice could not be measured clearly (data not shown). On the other hand, the free hemin accumulation was measured in the ultrafiltered plasma, from which hemoCD1 had been removed together with proteins by the ultrafiltration process. Figure 9a shows the changes in the free hemin concentration in the protein-depleted plasma of the hemoCD1-treated mice. Free hemin significantly increased upon the removal of endogenous CO by hemoCD1. The accumulation of free hemin was further evidenced by the subsequent down-regulation of ALAS-1 mRNA (*Alas1*) in the


DOI: 10.1021/jacs.6b02211
J. Am. Chem. Soc. 2016, 138, 5417−5425

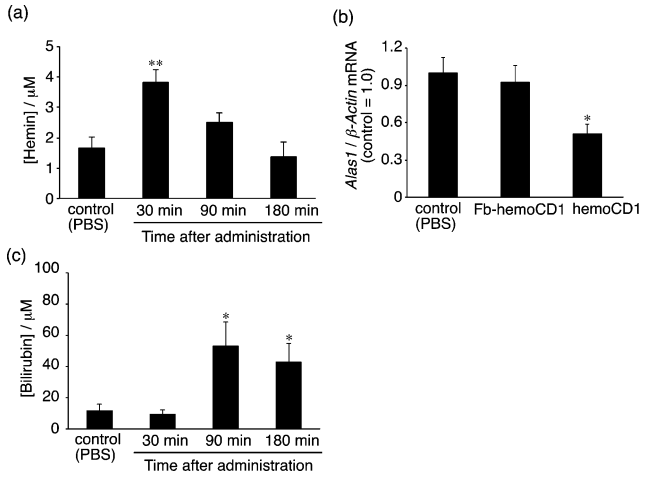


**Figure 9.** Accumulation of free hemin and bilirubin in the blood plasma of mice induced by CO-depletion. (a) Free hemin concentration in the protein-free plasma of mice after the administration of hemoCD1 (1.0 mM, 0.15 mL in PBS). The samples for the controls were obtained from the mice at 30 min after the intraperitoneal administration of PBS (0.15 mL). (b) The expression level of *Alas1* mRNA in the livers of mice at 90 min after the administration of hemoCD1 (1.0 mM, 0.15 mL in PBS). PBS and Fb-hemoCD1 were similarly administered as the negative controls. (c) Bilirubin concentration in the plasma of mice after the administration of hemoCD1 (1.0 mM, 0.15 mL in PBS). The samples for the controls were obtained from the mice at 30 min after the intraperitoneal administration of PBS (0.15 mL). Each bar represents the means ± SE ($n$ = 3–4 experiments per group). An asterisk denotes statistical significance; $^{*}P < 0.05$, $^{**}P < 0.01$, as compared to the controls.

liver (Figure 9b). ALAS-1 is the enzyme that produces δ-aminolevulinoic acid (ALA) for heme biosynthesis and it is known that the transcription system for this enzyme is inhibited by excess hemin.[50] The enhanced free hemin content in the plasma returned smoothly to a normal level (Figure 9a), suggesting the rapid degradation of hemin catalyzed by HO. In accordance with this, the concentration of bilirubin in the plasma was significantly increased (Figure 9c). The rise and decay in the time course of free hemin (Figure 9a) corresponded well with the depletion and recovery of CO-Hb, respectively, in the blood (Figure 6). In addition, the time course of the bilirubin concentration in the plasma (Figure 9c) appeared to be correlated to that of the *Hmox1* induction observed in the hemoCD-treated mice (Figure 7).

**A Feedback Mechanism in the CO/HO-1 System.** The present study revealed the relationship between the CO-depletion and the HO-1 induction in vivo. A plausible feedback mechanism is shown in Figure 10. The CO-removal from CO-Hb generates oxy-Hb. Oxy-Hb in RBC is very stable and is rarely oxidized to met-Hb because of the reduction system in the RBC membrane.[45] In contrast, cell-free oxy-Hb in the blood plasma is readily oxidized to met-Hb by ROS such as $H_2O_2$ and subsequently dissociates to hemin and apo-globin.[42] The oxidation of CO-Hb by $H_2O_2$ should proceed much slower even in the blood plasma, resulting in the slow metabolism of cell-free CO-Hb by HO. Accordingly, the CO-depletion by hemoCD1 in vivo caused an accumulation of free hemin in the blood plasma. The unusual content of free hemin induces expression of HO-1 to metabolize this excess. The newly produced CO binds to ferrous Hb to form CO-Hb as the

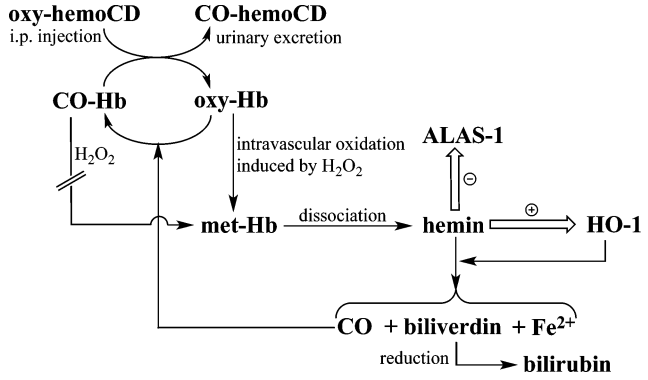


**Figure 10.** A homeostatic feedback model for the endogenous CO/HO-1 system in the blood plasma.

oxidation-resistant state, which restores the ferrous/ferric balance of cell-free Hb back to the homeostatic steady-state.

Endogenous CO contained in the whole blood and in the blood plasma from the untreated mice was quantified by the photometric assay using hemoCD1 (see Figure S7 in Supporting Information). We found that hemoCD1 could be used for quantification of endogenous CO in the blood because of its much higher CO affinity than Hb. Accordingly, $(2.2 \pm 0.2) \times 10^{-8}$ and $(9.2 \pm 0.6) \times 10^{-9}$ mol of CO were found in the whole blood and in the blood plasma, respectively. The amount of CO detected in the whole blood was consistent with that quantified by gas chromatography.[51] The assay revealed that 42 ± 4% of endogenous CO was found in the blood plasma, indicating that a significant amount of endogenous CO is supposed to bind to cell-free Hb in the blood plasma. Because hemoCD cannot penetrate the cell membrane, administered hemoCD removes endogenous CO primarily from cell-free CO-Hb in the blood plasma, leading to the feedback response as shown in Figure 10.

## ■ CONCLUSIONS

The present study demonstrated the production of a pseudoknockdown state of endogenous CO in mice using the supramolecular complexes, hemoCDs. The CO-depletion caused a temporal decrease in the amount of CO-Hb in the blood of treated mice, which induced HO-1. The induced HO-1 accelerated endogenous CO production to compensate for the reduced CO in the blood. To our knowledge, this is the first example showing that the lack of CO in the blood causes a feedback-driven compensatory up-regulation of HO-1 to maintain constant CO-Hb level in the blood. The in vivo and in vitro experiments revealed a regulatory role of CO in maintaining the balance between ferrous Hb and ferric met-Hb. The strong coordination of CO to ferrous Hb can suppress the oxidation of cell-free Hb to met-Hb that is promoted by $H_2O_2$. The CO-depletion in the blood resulted in the accumulation of free hemin, leading to rapid metabolism of free hemin by the HO enzyme to produce de novo endogenous CO. In summary, we have proposed a major regulatory role of endogenous CO in the blood through the use of hemoCDs. We believe that the present pseudoknockdown system will also be applicable for the investigation of other cryptic functions of CO in biological systems.

## ■ EXPERIMENTAL SECTION

**Sample Preparation.** $Fe^{III}$TPPS (2.75 mg, 2.0 μmol) and Py3CD (7.05 mg, 2.4 μmol)[26] were dissolved in PBS (1 mL) to yield a


DOI: 10.1021/jacs.6b02211
J. Am. Chem. Soc. 2016, 138, 5417–5425

solution of met-hemoCD1 (2 mM). The solutions of met-hemoCD2 and met-hemoCD3 were prepared as well using Py2CD[28] and Py3OCD.[29] To the solution of met-hemoCD was added $Na_2S_2O_4$ (ca. 1 mg) to reduce the met-hemoCD to ferrous hemoCD. Excess $Na_2S_2O_4$ was removed by passing the solution through a HiTrap desalting column (Sephadex G25, GE Healthcare Life Sciences). During this process under aerobic conditions, the ferrous hemoCDs bound $O_2$ in the air. The resulting solution containing ferrous hemoCD was appropriately diluted with PBS to obtain 0.5, 1.0, or 1.5 mM of the solution, the concentration of hemoCD being determined from its absorption coefficient as reported elsewhere.[29,33] A solution of Fb-hemoCD (1.0 mM) was prepared by dissolving TPPS (0.94 mg, 1.0 μmol) and Py3CD (3.52 mg, 1.2 μmol) in PBS (1 mL).

**Animal Experiments.** The experiments were carried out in accordance with the Guidelines for Animal Experiments of Doshisha University and of Doshisha Women's College of Liberal Arts. Male C57BL/6N mice weighing 20−22 g were used. The mice were housed under controlled environmental conditions and fed commercial feed pellets. All mice had free access to food and water.

A solution of hemoCD (0.15 mL) was intraperitoneally administrated to the subject mouse. The naturally excreted urine was collected (around 30 μL per 30 min), which was appropriately diluted with PBS and then measured by UV−vis spectroscopy (Shimadzu UV-2450). The assay for determining the amount of met-, oxy-, and CO complexes of hemoCD in the urine was described elsewhere.[29,31−33] The mice were sacrificed by cervical dislocation at 30, 90, and 180 min after the administration, and the liver was excised by disposable biopsy punch (5 mmϕ, Kai Medical), which was soaked in RNA later (Life Tech), and stored at 4 °C until use. For blood sampling, after the administration the mice were anaesthetized by isoflurane inhalation and the blood samples were collected from the postcava using a 23G syringe (Terumo). The blood samples were mixed with heparin and stored at −80 °C in the dark until use.

**Cell Cultures.** The human hepatoma cell line (HepG2) was obtained from RIKEN Cell Bank and cultured in Dulbecco's modified Eagle's medium (DMEM, Wako) supplemented with 10% fetal bovine serum (FBS, Invitrogen GIBCO, heat inactivated at 56 °C before use) and 1% penicillin/streptomycin/amphotericin B (Wako) at 37 °C in a humidified atmosphere with 5% $CO_2$. Cells were changed to serum-free medium (OPTI-MEM, Invitrogen GIBCO) before the treatments with agents. The cells were treated by hemoCD1, hemin (TCI, stock solution prepared using DMSO), human Hb (met-Hb was purchased from Sigma-Aldrich, ferrous Hb was prepared using $Na_2S_2O_4$ as a reducing agent, followed by purification using a HiTrap desalting column; the concentration of Hb was determined using reported absorption coefficients[52]), $H_2O_2$ (Wako), 1-hydroxy-2-oxo-3-(3-aminopropyl)-3-isopropyl-1-triazene (NOC, a NO releasing molecule, Dojin Chemicals) or their mixed systems as described in Figure 8. After the incubation with these agents for 2 h, the cells were washed well with PBS and total RNA was then extracted, which was used for RT-PCR (below).

**CO-Hb Content in Blood.** The amount of CO-Hb in the blood was measured according to the reported method.[53] The blood samples (0.5 mL) obtained from the mice after the intraperitoneal administration of hemoCD were placed in a 5 mL 25G syringe (Terumo) sealed with a septum cap (natural rubber, for a 7 mm tube). To this, 3-drops of 4% Triton X-100 and 3-drops of *n*-octanol were injected through the septum. The mixture was then mixed well using a 5 mmϕ glass ball. The atmosphere in the syringe (1 mL) was carefully replaced with He gas. Methane gas (10 μL) was added to the atmosphere through the septum in the syringe as an internal standard. Subsequently, 0.3 mL of 20% aqueous solution of $K_3[Fe(CN)_6]$ was added to oxidize the ferrous Hb, and the liberated CO from CO-Hb in the gas phase (0.5 mL) was analyzed by means of gas chromatography (GC, Shimadzu GC-2014). It was confirmed that the CO gas was not liberated from CO-hemoCD by this treatment (CO-hemoCD was hardly oxidized by excess $K_3[Fe(CN)_6]$ in the aqueous solution). The GC conditions were as follows: detector; TCD, column; SHINCARBON, carrier gas; He, column temperature; 40 °C, temperature at vaporizing chamber and detector: 120 °C; and flow rate: 50 mL/min. The content of CO-Hb in the whole blood was determined from the amount of CO determined by GC and the amount of total Hb, which was measured by the CN-met-Hb method as previously reported.[54]

**RT-PCR.** Total RNA was isolated from the mouse livers or HepG2 cells using the RNeasy Mini kit (Qiagen) according to the manufacturer's instructions. The RNA concentration and purity were determined by measuring the absorbances at 260 and 280 nm (Shimadzu BioSpec-nano). The resulting total RNA (1 μg) was reverse transcribed in a mixture (20 μL) of 5 × RT buffer (Toyobo, 4 μL), 10 mM dNTP (Toyobo, 2 μL), RNase Inhibitor (Toyobo, 1 μL), Oligo(dT)20 (Toyobo, 1 μL) and Rever Tra Ace (Toyobo, 1 μL). The sample was incubated at 30 °C for 10 min, at 42 °C for 20 min, and at 99 °C for 5 min. Real-time PCR was performed in a mixture (10 μL) of cDNA (1.0 ng/μL, 2 μL), forward and reverse primers (10 μM, 0.2 μL), distilled water (2.6 μL), and 2 × SYBR Green Master Mix (Applied Biosystems, 5 μL) using a Step One real time PCR system (Applied Biosystems). The primers are listed in Table S1. β-Actin was used as a reference gene. Forty cycles (95 °C for 30 s, 60 °C for 60 s) of PCR were performed after 10 min of denaturation at 95 °C. All samples were measured in triplicate. Data were analyzed by the relative standard curve method using StepOne software v2.3 (Applied Biosystems). Semiquantitative PCR was applied for the in vitro study. PCR was performed in a mixture of cDNA, PCR buffer (Toyobo), dNTP (Toyobo), forward and reverse primers, and DNA polymerase {KOD Dash (Toyobo) or Blend Taq (Toyobo)}. The primer sequences are listed in Table S2. The amplification reactions commenced with an initial denaturation step at 94 °C for 2 min, followed by denaturation at 94 °C for 1 min, annealing at 60 °C for 1 min, and extension at 72 °C for 2 min (15 cycles for KOD Dash, 21 cycles for blend-taq). For each reaction, a final extension of 72 °C for 5 min was carried out and the samples were then held at 4 °C until processed. The PCR products were analyzed by 2% agarose gel electrophoresis with ethidium bromide. The gel images were captured by a UV transilluminator (FAS-IV, Japan Genetics) and the band intensities were measured using the ImageJ software.

**Western Blot.** The mouse liver was homogenized in RIPA Lysis Buffer (ATTO, 20 mM HEPES, 150 mM NaCl, 1.0% IGEPAL CA-630, 0.1% SDS, and 0.5% sodium deoxycholate) after the additions of the protease inhibitor (ATTO) and phosphatase inhibitor (ATTO). The protein concentration was determined using a BCA Protein Assay Kit (Pierce). The protein sample (10 μL) was mixed with 2 × sample loading buffer (10 μL containing 4% SDS, 10% 2-mercaptoethanol, 20% glycerol, and 0.01% bromophenol blue in 125 mM Tris-HCl, pH 6.8), heated at 90 °C for 5 min, and separated by 12.5% SDS-PAGE. Proteins in the gels were electrophoretically transferred onto a polyvinylidene difluoride membrane at 144 mA for 50 min. The membrane was blocked with 5% skimmed milk in Tris buffer saline (TBS) for 1 h at room temperature. After washing the membrane with TBS-T (TBS containing 0.1% Tween), a polyclonal rabbit anti-HO-1 antibody (SPA-895, StressGen, 1:3000) was added and incubated overnight at 4 °C. The blots were incubated for 30 min at room temperature with HRP-conjugated secondary antibody (NA-931, Amersham Biosciences, 1:5000). Blots were processed with an ECL kit (Pierce) and the chemiluminescence signal was detected using an LAS-3000 mini image analyzer (Fuji Photo Film).

**Quantification of Free Hemin in the Plasma.** The concentration of free hemin in the blood plasma was measured according to the reported method.[47] After centrifuging the blood samples obtained from the mice (4 °C, 400*g*, 20 min), the plasma solution was collected and passed through an Amicon Ultra Centrifugal filter units (0.5 mL, MWCO 3000, centrifuged at 15 °C and 15 000*g* for 60 min) to remove proteins as well as hemoCD. The concentration of free hemin in the protein-depleted plasma was quantified by a chromogenic assay according to the manufacturer's instructions (QuantiChrom heme assay kit, Bioassay Systems). The colorimetric change was monitored at 405 nm using a Filter Max F5 plate reader (Molecular Devices).

**Quantification of Bilirubin in the Plasma.** The amount of bilirubin in the blood plasma was measured according to the reported method.[55−57] After the centrifugation (4 °C, 400*g*, 20 min) of the blood sample obtained from the treated mice, the plasma solution (0.1


DOI: 10.1021/jacs.6b02211
J. Am. Chem. Soc. 2016, 138, 5417−5425

mL) was diluted 10-fold with PBS. To the solution (1 mL) was added recombinant his-tagged UnaG[57] (0.24 mM aqueous solution, 15 μL) and then the solution was incubated for 2 h at 25 °C in the dark, after which the UnaG was trapped with Ni-NTA agarose (Invitrogen). After washing the resin with PBS, the UnaG was eluted with PBS containing 300 mM imidazole (300 μL). The fluorescence from the bilirubin-bound UnaG was monitored using a Filter Max F5 plate reader (Molecular Devices, $\lambda_{ex}$ = 485 ± 20 nm and $\lambda_{em}$ = 535 ± 25 nm).

**Statistical Analysis.** All data represent the means ± SE from at least three different experiments. Statistical analysis ($n \geq 3$) was performed by using an unpaired Student's *t*-test. The *P* value less than 0.05 was considered significant.

## ■ ASSOCIATED CONTENT

### Supporting Information

The Supporting Information is available free of charge on the ACS Publications website at DOI: 10.1021/jacs.6b02211.

The primer sequences used for the RT-PCR experiments (Table S1 and S2), in vitro competitive reaction assay for Hb and hemoCD (Figure S1), time-courses of the molar fractions of oxy-, CO-, and met-hemoCD1 contained in the urine of the hemoCD1-treated mice (Figure S2), UV−vis spectra of TPPS, Fb-hemoCD, and the urine solution obtained after the intraperitoneal administration of Fb-hemoCD (Figure S3), mRNA expression levels of HO-2 (*Hmox2*) in the livers of mice after the administration of hemoCD1 (Figure S4), the UV−vis spectra for the reaction of oxy- and CO-Hb with $H_2O_2$ (Figure S5) and with NO (Figure S6) in aqueous solutions, and the photometric assay for the quantification of endogenous CO by hemoCD1 in the blood (Figure S7). (PDF)

## ■ AUTHOR INFORMATION


### Corresponding Author

*hkitagis@mail.doshisha.ac.jp


### Notes

The authors declare no competing financial interest.

## ■ ACKNOWLEDGMENTS

This work was financially supported by a Grant-in-Aid for Young Scientists (B) (No. 26870704) from the Japan Society for the Promotion of Science (JSPS), the MEXT-Supported Program for the Strategic Research Foundation at Private Universities (2015−2019), and The Uehara Memorial Foundation.

## ■ REFERENCES


(1) Wu, L.; Wang, R. *Pharmacol. Rev.* **2005**, *57*, 585−630.
(2) Ryter, S. W.; Alam, J.; Choi, A. M. *Physiol. Rev.* **2006**, *86*, 583−650.
(3) Rother, R. P.; Bell, L.; Hillmen, P.; Gladwin, M. T. *JAMA* **2005**, *293*, 1653−1662.
(4) Balla, J.; Vercellotti, G. M.; Jeney, V.; Yachie, A.; Varga, Z.; Eaton, J. W.; Balla, G. *Mol. Nutr. Food Res.* **2005**, *49*, 1030−1043.
(5) Ferreira, A.; Balla, J.; Jeney, V.; Balla, G.; Soares, M. P. *J. Mol. Med.* **2008**, *86*, 1097−1111.
(6) Piantadosi, C. A. *Antioxid. Redox Signaling* **2002**, *4*, 259−270.
(7) Coburn, R. F. *Ann. N. Y. Acad. Sci.* **1970**, *174*, 11−22.
(8) Miró, Ò.; Alonso, J. R.; Jarreta, D.; Casademont, J.; Urbano-Márquez, Á.; Cardellach, F. *Carcinogenesis* **1999**, *20*, 1331−1336.
(9) Sato, K.; Balla, J.; Otterbein, L.; Smith, R. N.; Brouard, S.; Lin, Y.; Csizmadia, E.; Sevigny, J.; Robson, S. C.; Vercellotti, G.; Choi, A. M.; Bach, F. H.; Soares, M. P. *J. Immunol.* **2001**, *166*, 4185−4194.
(10) Amersi, F.; Shen, X. D.; Anselmo, D.; Melinek, J.; Iyer, S.; Southard, D. J.; Katori, M.; Volk, H. D.; Busuttil, R. W.; Buelow, R.; Kupiec-Weglinski, J. W. *Hepatology* **2002**, *35*, 815−823.
(11) Johnson, T. R.; Mann, B. E.; Clark, J. E.; Foresti, R.; Green, C. J.; Motterlini, R. *Angew. Chem., Int. Ed.* **2003**, *42*, 3722−3729.
(12) Motterlini, R.; Otterbein, L. E. *Nat. Rev. Drug Discovery* **2010**, *9*, 728−743.
(13) Romão, C. C.; Blättler, W. A.; Seixas, J. D.; Bernardes, G. J. L. *Chem. Soc. Rev.* **2012**, *41*, 3571−3583.
(14) Heinemann, S. H.; Hoshi, T.; Westerhausen, M.; Schiller, A. *Chem. Commun.* **2014**, *50*, 3644−3660.
(15) Nikam, A.; Ollivier, A.; Rivard, M.; Wilson, J. L.; Mebarki, K.; Martens, T.; Dubois-Randé, J.-L.; Motterlini, R.; Foresti, R. *J. Med. Chem.* **2016**, *59*, 756−762.
(16) Otterbein, L. E.; Bach, F. H.; Alam, J.; Soares, M.; Tao, L. H.; Wysk, M.; Davis, R. J.; Flavell, R. A.; Choi, A. M. *Nat. Med.* **2000**, *6*, 422−428.
(17) Morse, D.; Pischke, S. E.; Zhou, Z.; Davis, R. J.; Flavell, R. A.; Loop, T.; Otterbein, S. L.; Otterbein, L. E.; Choi, A. M. K. *J. Biol. Chem.* **2003**, *278*, 36993−36998.
(18) Bilban, M.; Bach, F. H.; Otterbein, S. L.; Ifedigbo, E.; d'Avila, J. C.; Esterbauer, H.; Chin, B. Y.; Usheva, A.; Robson, S. C.; Wagner, O.; Otterbein, L. E. *Immunity* **2006**, *24*, 601−610.
(19) Nakahira, K.; Kim, H. P.; Geng, X. H.; Nakao, A.; Wang, X.; Murase, N.; Drain, P. F.; Wang, X.; Sasidhar, M.; Nabel, E. G.; Takahashi, T.; Lukacs, N. W.; Ryter, S. W.; Morita, K.; Choi, A. M. *J. Exp. Med.* **2006**, *203*, 2377−2389.
(20) Dioum, E. M.; Rutter, J.; Tuckerman, J. R.; Gonzalez, G.; Gilles-Gonzalez, M. A.; McKnight, S. L. *Science* **2002**, *298*, 2385−2387.
(21) Aono, S. *Acc. Chem. Res.* **2003**, *36*, 825−831.
(22) Boehning, D.; Snyder, S. H. *Science* **2002**, *298*, 2339−2340.
(23) Hou, S.; Reynolds, M. F.; Horrigan, F. T.; Heinemann, S. H.; Hoshi, T. *Acc. Chem. Res.* **2006**, *39*, 918−924.
(24) Yachie, A.; Niida, Y.; Wada, T.; Igarashi, N.; Kaneda, H.; Toma, T.; Ohta, K.; Kasahara, Y.; Koizumi, S. *J. Clin. Invest.* **1999**, *103*, 129−135.
(25) Morikawa, T.; Kajimura, M.; Nakamura, T.; Hishiki, T.; Nakanishi, T.; Yukutake, Y.; Nagahata, Y.; Ishikawa, M.; Hattori, K.; Takenouchi, T.; Takahashi, T.; Ishii, I.; Matsubara, K.; Kabe, Y.; Uchiyama, S.; Nagata, E.; Gadalla, M. M.; Snyder, S. H.; Suematsu, M. *Proc. Natl. Acad. Sci. U. S. A.* **2012**, *109*, 1293−1298.
(26) Kano, K.; Kitagishi, H.; Kodera, M.; Hirota, S. *Angew. Chem., Int. Ed.* **2005**, *44*, 435−438.
(27) Kano, K.; Kitagishi, H.; Dagallier, C.; Kodera, M.; Matsuo, T.; Hayashi, T.; Hisaeda, Y.; Hirota, S. *Inorg. Chem.* **2006**, *45*, 4448−4460.
(28) Kano, K.; Itoh, Y.; Kitagishi, H.; Hayashi, T.; Hirota, S. *J. Am. Chem. Soc.* **2008**, *130*, 8006−8015.
(29) Watanabe, K.; Kitagishi, H.; Kano, K. *Angew. Chem., Int. Ed.* **2013**, *52*, 6894−6897.
(30) Collman, J. P.; Boulatov, R.; Sunderland, C. J.; Fu, L. *Chem. Rev.* **2004**, *104*, 561−588.
(31) Kitagishi, H.; Negi, S.; Kiriyama, A.; Honbo, A.; Sugiura, Y.; Kawaguchi, A. T.; Kano, K. *Angew. Chem., Int. Ed.* **2010**, *49*, 1312−1315.
(32) Ueda, T.; Kitagishi, H.; Kano, K. *Org. Biomol. Chem.* **2012**, *10*, 4337−4347.
(33) Kano, K.; Chimoto, S.; Tamaki, M.; Itoh, Y.; Kitagishi, H. *Dalton Trans.* **2012**, *41*, 453−461.
(34) Matthew, E.; Warden, G.; Dedman, J. *Am. J. Physiol. Lung Cell. Mol. Physiol.* **2001**, *280*, L716−L723.
(35) Kitagishi, H.; Minami, K.; Kano, K. *Chem. Lett.* **2014**, *43*, 1095−1097.
(36) Mitrione, S. M.; Villalon, P.; Lutton, J. D.; Levere, R. D.; Abraham, N. G. *Am. J. Med. Sci.* **1988**, *296*, 180−186.
(37) Shirataki, C.; Shoji, O.; Terada, M.; Ozaki, S.-i.; Sugimoto, H.; Shiro, Y.; Watanabe, Y. *Angew. Chem., Int. Ed.* **2014**, *53*, 2862−2866.
(38) Karasugi, K.; Kitagishi, H.; Kano, K. *Bioconjugate Chem.* **2012**, *23*, 2365−2376.




DOI: 10.1021/jacs.6b02211
J. Am. Chem. Soc. 2016, 138, 5417−5425

(39) Ghattas, M. H.; Chuang, L. T.; Kappas, A.; Abraham, N. G. *Int. J. Biochem. Cell Biol.* **2002**, *34*, 1619−1628.
(40) Sun, J.; Hoshino, H.; Takaku, K.; Nakajima, O.; Muto, A.; Suzuki, H.; Tashiro, S.; Takahashi, S.; Shibahara, S.; Alam, J.; Taketo, M. M.; Yamamoto, M.; Igarashi, K. *EMBO J.* **2004**, *21*, 5216−5224.
(41) Hargrove, M. S.; Olson, J. S. *Biochemistry* **1996**, *35*, 11310−11318.
(42) Gladwin, M. T.; Kanias, T.; Kim-Shapiro, D. B. *J. Clin. Invest.* **2012**, *122*, 1205−1208.
(43) Varma, S. D.; Devamanoharan, P. S. *Free Radical Res. Commun.* **1991**, *14*, 125−131.
(44) Kelm, M. *Biochim. Biophys. Acta, Bioenerg.* **1999**, *1411*, 273−289.
(45) Shikama, K. *Chem. Rev.* **1998**, *98*, 1357−1373.
(46) Yusa, K.; Shikama, K. *Biochemistry* **1987**, *26*, 6684−6688.
(47) Pamplona, A.; Ferreira, A.; Balla, J.; Jeney, V.; Balla, G.; Epiphanio, S.; Chora, Â.; Rodrigues, C. D.; Gregoire, I. P.; Cunha-Rodrigues, M.; Portugal, S.; Soares, M. P.; Mota, M. M. *Nat. Med.* **2007**, *13*, 703−710.
(48) Tsai, A. L.; Berka, V.; Martin, E.; Olson, J. S. *Biochemistry* **2012**, *51*, 172−186.
(49) Herold, S.; Röck, G. *Biochemistry* **2005**, *44*, 6223−6231.
(50) Yamamoto, M.; Kure, S.; Engel, J. D.; Hiraga, K. *J. Biol. Chem.* **1988**, *263*, 15973−15979.
(51) The amount of endogenous CO was estimated by gas chromatography to be $2.66 \times 10^{-8}$ mol in the whole blood, where [Hb] = 7.4 mM (as monomer); the fraction of CO-Hb, 0.2%; blood volume, 1.8 mL.
(52) Antonini, E.; Brunori, M. Hemoglobin and myoglobin in their reactions with ligands. In *Frontiers in Biology*; Neuberger, A., Tatum, E. L., Ed.; Elsevier: Amsterdam, 1971; Chapter 13.
(53) Vreman, H. J.; Kwong, L. K.; Stevenson, D. K. *Clin. Chem.* **1984**, *30*, 1382−1386.
(54) Rodkey, F. L.; Hill, T. A.; Pitts, L. L.; Robertson, R. F. *Clin. Chem.* **1979**, *25*, 1388−1393.
(55) Takeda, T. A.; Mu, A.; Tai, T. T.; Kitajima, S.; Taketani, S. *Sci. Rep.* **2015**, *5*, 10488.
(56) Liem, P. H.; Mu, A.; Kikuta, S.-i.; Ohta, K.; Kitajima, S.; Taketani, S. *Biol. Chem.* **2015**, *396*, 1265−1268.
(57) Kumagai, A.; Ando, R.; Miyatake, H.; Greimel, P.; Kobayashi, T.; Hirabayashi, Y.; Shimogori, T.; Miyawaki, A. *Cell* **2013**, *153*, 1602−1611.


DOI: 10.1021/jacs.6b02211
*J. Am. Chem. Soc.* 2016, 138, 5417−5425